# ARTICLES

## Investigation of the $S_1$/ICT → $S_0$ Internal Conversion Lifetime of 4′-apo-β-caroten-4′-al and 8′-apo-β-caroten-8′-al: Dependence on Conjugation Length and Solvent Polarity

**Florian Ehlers,[†] Duncan A. Wild,[†] Thomas Lenzer,*[,†,‡] and Kawon Oum*[,‡]**

*Max-Planck-Institut für biophysikalische Chemie, Abt. Spektroskopie und Photochemische Kinetik (10100), Am Fassberg 11, D-37077 Göttingen, Germany, and Institut für Physikalische Chemie, Universität Göttingen, Tammannstrasse 6, D-37077 Göttingen, Germany*

*Received: November 19, 2006; In Final Form: February 1, 2007*

The ultrafast internal conversion (IC) dynamics of aldehyde-substituted apocarotenoids (*n*′-apo-β-caroten-*n*′-als with $n = 4$, 8 and 12) have been investigated in a systematic variation of conjugation length and solvent polarity using time-resolved femtosecond transient absorption spectroscopy. After excitation to the $S_2$ state with different excess energies, the subsequent intramolecular dynamics were investigated at several probe wavelengths covering the $S_0 \rightarrow S_2$ and $S_1$/ICT → $S_n$ absorption bands. Time constants $\tau_1$ for the internal conversion process $S_1$/ICT → $S_0$ of 4′-apo-β-caroten-4′-al and 8′-apo-β-caroten-8′-al have been newly measured. We compared these results with our earlier measurements for 12′-apo-β-caroten-12′-al (D.A. Wild, K. Winkler, S. Stalke, K. Oum, T. Lenzer *Phys. Chem. Chem. Phys.* **2006**, *8*, 2499). In the case of the aldehyde with the longest conjugation (4′-apo-β-caroten-4′-al), $\tau_1$ is almost independent of solvent polarity (4−5 ps), whereas a significant reduction of $\tau_1$ from 22.7 to 8.6 ps for the shorter 8′-apo-β-caroten-8′-al and an even more pronounced reduction from 220 to 8.0 ps for 12′-apo-β-caroten-12′-al were observed when the solvent medium was changed from *n*-hexane to methanol, respectively. In *n*-hexane, $\tau_1$ of the apocarotenals is strongly dependent on the conjugation length and this can be well understood in terms of an energy gap law description where the $S_1-S_0$ energy differences were estimated from their steady-state fluorescence spectra. In highly polar solvents, the IC to $S_0$ is very fast, irrespective of the conjugation length. This is probably due to the stabilization of an intramolecular charge transfer (ICT) state in 12′-apo-β-caroten-12′-al and 8′-apo-β-caroten-8′-al. In the case of 4′-apo-β-caroten-4′-al, such an influence of an ICT state is presumably less important than for the other two apocarotenals.

### 1. Introduction

Carotenoids fulfill several important roles in nature. For instance, in photosynthesis they serve as light-harvesting pigments in the blue-green spectral region.[1,2] Another function is protection against excessive light, which is accomplished by quenching both singlet and triplet states of bacteriochlorophylls.[3] Carotenoids with carbonyl substituents attached to the conjugated system, like peridinin or fucoxanthin, constitute a very important subclass. Peridinin is found in large amounts in oceanic dinoflagellates[4−7] and is the main light-harvesting pigment in the peridinin-chlorophyll-a-protein (PCP) complex.[8] Because of this function and the unusual solvent dependence of the lifetime of peridinin's first excited electronic state in solvents of different polarity, it has recently attracted considerable attention.[9−18]

The main route of the radiationless processes in carotenoids after photoexcitation can be described by a few low-lying electronically excited states. The first excited singlet state $S_1(2^1A_g^-)$ cannot be populated by a one-photon transition from the electronic ground state $S_0(1^1A_g^-)$ because it is symmetry forbidden (labels are based on idealized $C_{2h}$ polyene symmetry, which are useful even for more asymmetric carotenoids, because their properties are mainly determined by the structure of their conjugated system). The strong absorption band located in the visible region of the spectrum is due to the transition to the second electronically excited singlet state $S_2(1^1B_u^+)$. After one-photon excitation to $S_2$ the dynamics are governed by ultrafast internal conversion (IC) processes, and typical lifetimes $\tau_2$ for the $S_2 \rightarrow S_1$ transition are extremely short, on the order of <200 fs. In contrast, the IC process $S_1 \rightarrow S_0$ is usually much slower, with relaxation time constants $\tau_1$ on the order of picoseconds to nanoseconds. The presence of additional dark states has also been proposed. However, the direct experimental identification of these states, denoted as $1^1B_u^-$, $3^1A_g^-$,[19,20] $S_x$,[21] $S^‡$,[22] or $S^*$,[23−27] and their role in relaxation pathways of excited carotenoids are still under debate.[2,28]

Especially, studies of $S_1$ lifetimes of carotenoids have been extensively carried out by several research groups, since Wasielewski and Kispert reported the first measurement of the $S_1$ lifetimes of carotenoids (β-carotene, canthaxanthin and 8′-apo-β-caroten-8′-al) in 1986.[29] The $S_1$ lifetime is a good indicator of the role of conjugation length, solvent polarity,

* Corresponding author. Tel: +49 551 3912598. Fax: +49 551 393150. E-mails: tlenzer@gwdg.de, koum@gwdg.de.
† Max-Planck-Institut für biophysikalische Chemie.
‡ Universität Göttingen.

10.1021/jp0676888 CCC: $37.00 
Published on Web 03/07/2007

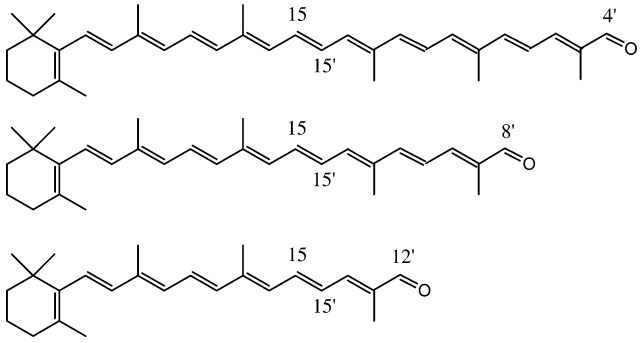


**Figure 1.** Structures of 4′-apo-$\beta$-caroten-4′-al, 8′-apo-$\beta$-caroten-8′-al, and 12′-apo-$\beta$-caroten-12′-al (from top to bottom).

excitation wavelength, terminal groups, etc., in the excited-state dynamics of carotenoids (see, e.g., the review by Polívka and Sundström[2] and the references cited therein). For unsubstituted carotenoids, the $S_1$ lifetime depends primarily on the conjugation length. Especially for some $C_{40}$ carotenoids (such as $\beta$-carotene, lycopene, (3*R*,3′*R*)-zeaxanthin, and (3*R*,3′*R*,6′*R*)-lutein), the $S_1$ lifetimes were found to be independent of solvent polarity.[30] When electron-withdrawing substituents, such as cyano groups in 7′,7′-dicyano-7′-apo-$\beta$-carotene[31] or a carbonyl group in peridinin[9,17,18] or 12′-apo-$\beta$-caroten-12′-al[32] were introduced, the excited-state dynamics of those carotenoids became more complicated, mainly due to the influence of additional excited states such as an intramolecular charge transfer (ICT) state, which can be stabilized by polar solvent environments. Therefore, it is not straightforward to compare the lifetimes only in terms of conjugation length, but one also has to consider the influence of different experimental conditions, such as solvent properties, different excitation energies, terminal groups, etc.

It is therefore our interest in this paper to present a systematic study of a series of apocarotenals (Figure 1), with special emphasis on the dependence on conjugation length and solvent polarity. We investigate the ultrafast internal conversion dynamics of 4′-apo-$\beta$-caroten-4′-al for the first time. Also, we report new time-resolved data for 8′-apo-$\beta$-caroten-8′-al, which is compared with previous data from other groups[29,31,33] and our earlier measurements for 12′-apo-$\beta$-caroten-12′-al.[32] We also report steady-state fluorescence and absorption spectra to complement the time-resolved data.

## 2. Experimental Section

The experimental setup is an extended version of the one already described in our previous publication.[32] In short, the output of a Ti:sapphire oscillator-regenerative amplifier system (780 nm, 1 kHz, 1 mJ pulse$^{-1}$) was split up into two beams for pumping two home-built blue-pumped two-stage noncollinearly phase-matched optical parametric amplifiers (NOPA) delivering the pump and probe beams for the experiment.[34−36] The output of each NOPA was subsequently compressed by a pair of quartz prisms. This way 4′-apo-$\beta$-caroten-4′-al could be excited at the pump wavelengths 480 and 510 nm in the $S_0 \rightarrow S_2$ band. The subsequent dynamics were monitored either at the probe wavelength 510 nm ($S_0 \rightarrow S_2$ transition, ground state recovery, GSR) or at 610 nm, which is located on the carotenoid $S_1$/ICT $\rightarrow S_n$ excited-state absorption (ESA) band. For the measurements of 8′-apo-$\beta$-caroten-8′-al in different solvents, the molecules were excited at 390 nm by frequency-doubling the output of the Ti:sapphire laser in a BBO crystal to excite the molecule into higher vibrational levels of the $S_2$ state. The dynamics were subsequently probed either by frequency-doubling the output of the Ti:sapphire laser in a BBO crystal (390 nm, $S_0 \rightarrow S_2$) or by using one of the NOPAs tuned to a wavelength of 475 ($S_0 \rightarrow S_2$) or 630 nm ($S_1$/ICT $\rightarrow S_n$).

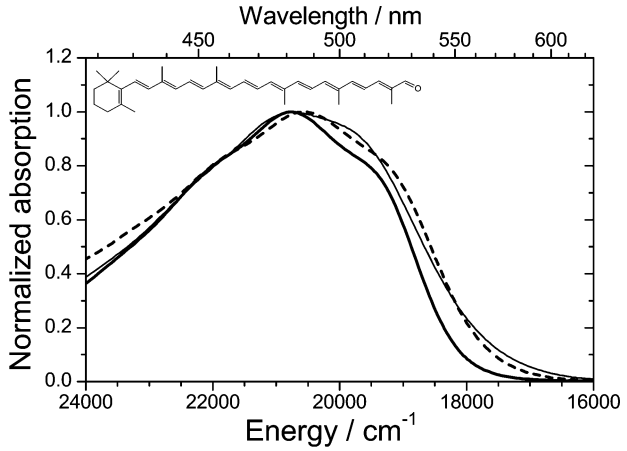


**Figure 2.** Normalized $S_0 \rightarrow S_2$ steady-state absorption spectra of 4′-apo-$\beta$-caroten-4′-al in *n*-hexane (thick solid line), tetrahydrofuran (dashed line) and methanol (thin solid line). The wavelength scale is shown on top for reference.

A computer-controlled delay stage served to delay the pump and probe pulses with respect to each other. Each beam was then attenuated and weakly focused into the sample cell under a small angle (diameter of the light spot approximately 250 $\mu$m). The relative polarizations of the pump and probe beams were adjusted to 54.7° (magic angle) to avoid any contributions from orientational relaxation. Probe energies were measured by two photodiodes, which were located in front of and behind the flow quartz cuvette (1 mm path length), which contained the apocarotenal solution. A chopper wheel was used to block every second pump pulse. The change in optical density ($\Delta$OD) was then given as

$$\Delta\mathrm{OD} = \mathrm{OD}_{\mathrm{exc}} - \mathrm{OD}_0 = \ln(I/I_0)_0 - \ln(I/I_0)_{\mathrm{exc}} \qquad (1)$$

Here, $\mathrm{OD}_{\mathrm{exc}}$ and $\mathrm{OD}_0$ are the optical densities with and without the pump beam, respectively. $(I/I_0)_{\mathrm{exc}}$ and $(I/I_0)_0$ are the ratios of the light intensities behind and in front of the cuvette with and without the pump beam. Typically, 4000−16000 laser shots were averaged for each delay time. The time resolution of the setup was between 100 and 150 fs. Pulse energies for the pump and probe beams were 2 $\mu$J or less. The carotenoid concentration was typically between 2.5 and 7.5 $\times$ 10$^{-5}$ M. Small coherence artefacts were found for some of the measurements within the cross-correlation of the pump and probe pulses. They have no influence on the time constants $\tau_1$ reported below. All-*trans* (all-*E*) samples of 4′-apo-$\beta$-caroten-4′-al, 8′-apo-$\beta$-caroten-8′-al and 12′-apo-$\beta$-caroten-12′-al were generously provided by BASF AG. The latter two were used directly, whereas 4′-apo-$\beta$-caroten-4′-al was post-purified by preparative HPLC, yielding purities >97% in all cases. All solvents had a purity ≥ 99%. Steady-state absorption and fluorescence spectra of 4′-apo-$\beta$-caroten-4′-al, 8′-apo-$\beta$-caroten-8′-al and 12′-apo-$\beta$-caroten-12′-al were recorded on a Varian Cary 5E and a Horiba Jobin Yvon FluoroLog-3 spectrometer, respectively.

## 3. Results and Discussion

**Steady-State Absorption and Fluorescence Spectra of Apocarotenals in Different Solvents.** Normalized $S_0 \rightarrow S_2$ steady-state absorption spectra of 4′-apo-$\beta$-caroten-4′-al in *n*-hexane, tetrahydrofuran, and methanol can be found in Figure 2. In Figures 3 and 4, we compare the absorption and fluorescence spectra of the 4′-, 8′- and 12′-species in *n*-hexane

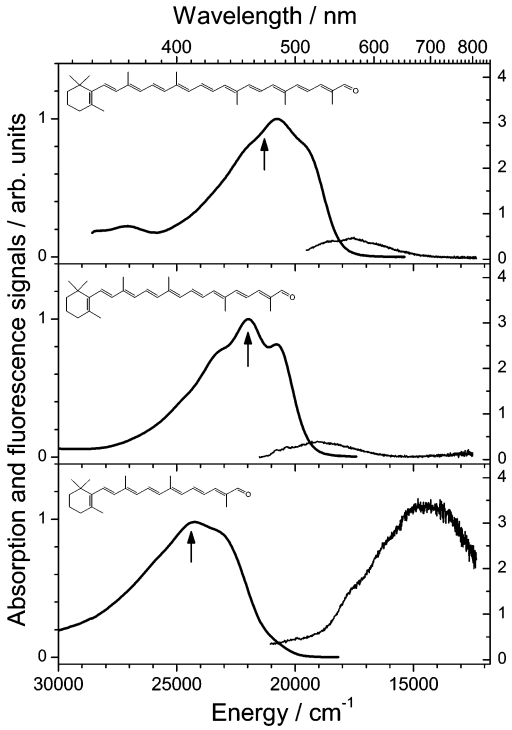


**Figure 3.** Room-temperature absorption (thick solid line) and fluorescence (thin solid line) spectra of 4′-apo-β-caroten-4′-al (top), 8′-apo-β-caroten-8′-al (middle), and 12′-apo-β-caroten-12′-al (bottom) in *n*-hexane. The excitation wavelength of each fluorescence spectrum is marked by an arrow. The wavelength scale is shown on top as a reference. The absorption spectra are normalized to 1 (graduation on the left axis), whereas the fluorescence spectra show the measured relative amplitudes (graduation on the right axis) and therefore allow a direct comparison of the amplitude of the three fluorescence bands.

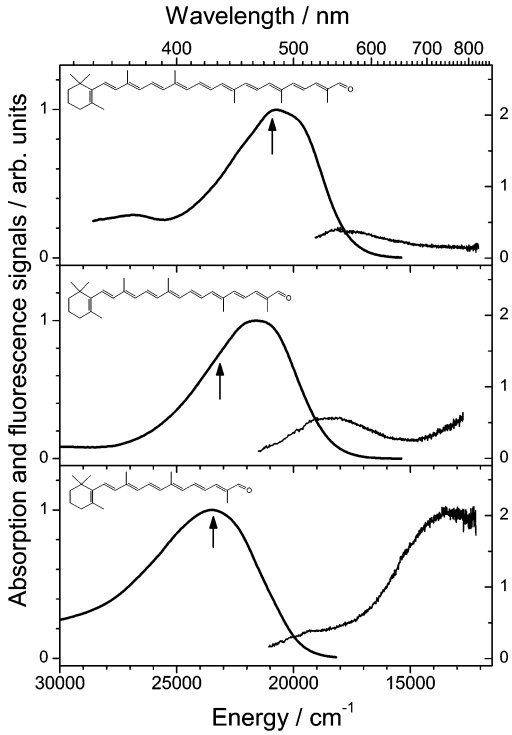


**Figure 4.** Room-temperature absorption (thick solid line) and fluorescence (thin solid line) spectra of 4′-apo-β-caroten-4′-al (top), 8′-apo-β-caroten-8′-al (middle), and 12′-apo-β-caroten-12′-al (bottom) in methanol. The excitation wavelength of each fluorescence spectrum is marked by an arrow. The wavelength scale is shown on top as a reference. The absorption spectra are normalized to 1 (graduation on the left axis), whereas the fluorescence spectra show the measured relative amplitudes (graduation on the right axis) and therefore allow a direct comparison of the amplitude of the three fluorescence bands.

and methanol, respectively. In addition, Table 1 gives an overview of the absorption maxima $\lambda_{max}$. The larger red shift of the $S_0 \rightarrow S_2$ absorption spectrum for longer carotenoids ($\Delta\lambda = 20-28$ nm, depending on the solvent) is consistent with earlier studies, and shows that the $S_0-S_2$ energy gap is strongly affected by the change of conjugation length.[31,37]

In *n*-hexane (see Figure 3), the vibronic structure of the $S_0 \rightarrow S_2$ absorption band of 8′-apo-β-caroten-8′-al is more resolved than that of the shorter conjugated 12′-species.[32] Interestingly, the absorption band is less structured for the longer 4′-species. Christensen et al. found a similar trend in their steady-state absorption spectra of seven apo-β-carotenes with different conjugation lengths ($N = 5-11$) in an ether/isopentane/ethanol matrix at 77 K.[37] In general, the conjugation length $N$ can be expressed as follows:

$$N = N_{\text{chain}} + N_{\beta} + N_{\text{aldehyde}} \qquad (2)$$

where $N_{\text{chain}}$ is the number of conjugated C=C double bonds in the polyene chain, $N_{\beta}$ is the number of C=C double bonds in β-ionone rings conjugated with the polyene chain, and $N_{\text{aldehyde}}$ is the number of aldehyde groups in conjugation with the polyene chain. Christensen et al.[37] observed a substantial sharpening of the vibronic structure in the absorption band when going from 12′-apo-β-carotene ($N = 7$) to 8′-apo-β-carotene ($N = 9$) but a slight re-broadening when going to 4′-apo-β-carotene ($N = 11$). To explain this observation, the authors suggested a "distribution of conformers" model: The nonplanarity between the double bond in the β-ionone ring and the polyene backbone is believed to have a smaller impact on the spread in transition energies when the conjugation length of the polyene chain is increased. Optical excitation of longer carotenes would therefore select conformers with a less heterogeneous distribution of $S_0 \rightarrow S_2$ transition energies.[37] The observation of the slight loss of vibronic structure for the 4′-species (both 4′-apo-β-carotene and 4′-apo-β-caroten-4′-al), however, cannot be explained by this model alone.

The solvent dependence of the steady-state absorption spectra of apocarotenals in this work is consistent with earlier observations made for structurally similar carotenoids.[31] The energetic position of the maximum and the bandwidth of the absorption band of carotenoids depend strongly on the solvent medium. Solvent-induced absorption spectral shifts of the $S_0 \rightarrow S_2$ transition of some $C_{40}$ carotenoids (β-carotene and astaxanthin) depend more on the solvent polarizability than the polarity, and the energetic position of the absorption band maximum of carotenoids is well correlated with the Lorentz-Lorenz function $R(n) = (n^2 - 1)/(n^2 + 2)$ of the refractive index of the solvent (for $R(n)$ values[38] see Table 1).[39] For apocarotenals, the influence of solvent polarity on the spectral shift becomes more pronounced. A loss of vibrational structure and an asymmetric broadening of the band toward longer wavelengths is found even in weakly polarizable polar hydrogen-bonding solvents like methanol (see Figures 2 and 4). This effect can be explained by a dipolar character of the electronic ground state $S_0$. In polar solvents, stabilization of the negative partial charge on the carbonyl oxygen leads to a broader distribution of conformers and therefore a loss of vibrational structure and an additional broadening of the spectra.[7,15,18] In addition, an increased mixing of charge-transfer character into the $S_2$ state of extended polyene systems has been suggested to contribute to this broadening.[31,40]

**TABLE 1: Lifetimes $\tau_1(S_1/ICT \rightarrow S_0)$ of 4′-apo-$\beta$-caroten-4′-al and 8′-apo-$\beta$-caroten-8′-al in Various Solvents at 298 K**

| solvent | $\lambda_{max}$ (nm)[a] | $R(n)$[b] | $R(\epsilon)$[b] | $\Delta f$[b] | $\lambda_{pump}$ (nm) | $\lambda_{probe}$ (nm) | $\tau_1$ (ps)[c] | ref |
|---|---|---|---|---|---|---|---|---|
| | | | | 4′-apo-$\beta$-caroten -4′-al | | | | |
| *n*-hexane | 482 | 0.23 | 0.23 | 0 | 480 | 510 | 4.6 | this paper |
| | | | | | | 610 | 4.7 | |
| | | | | | 510 | 510 | 4.8 | |
| | | | | | | 610 | 4.6 | |
| tetrahydrofuran | 486 | 0.25 | 0.69 | 0.44 | 480 | 510 | – | this paper |
| | | | | | | 610 | 5.1 | |
| | | | | | 510 | 510 | 4.9 | |
| | | | | | | 610 | 5.1 | |
| methanol | 483 | 0.20 | 0.91 | 0.71 | 480 | 510 | 3.8 | this paper |
| | | | | | | 610 | 4.2 | |
| | | | | | 510 | 510 | 3.8 | |
| | | | | | | 610 | 4.2 | |
| | | | | 8′-apo-$\beta$-caroten -8′-al | | | | |
| *n*-hexane | 454 | 0.23 | 0.23 | 0 | 390 | 390 | 21.0 | this paper |
| | | | | | | 475 | 25.4 | |
| | | | | | | 630 | 21.8 | |
| 3-methylpentane | – | 0.23 | 0.23 | 0 | 490 | 555 | 26.4 | 33,31 |
| toluene | – | 0.29 | 0.31 | 0.02 | 510 | 480 | 25.1 | 29 |
| tetrahydrofuran | 463 | 0.25 | 0.69 | 0.44 | 390 | 390 | 21.4 | this paper |
| | | | | | | 475 | 26.7 | |
| | | | | | | 630 | 25.0 | |
| dichloromethane | – | 0.26 | 0.73 | 0.47 | 490 | $S_1 \rightarrow S_n$[d] | 14.1 | 33 |
| ethanol | – | 0.22 | 0.89 | 0.67 | 490 | $S_1 \rightarrow S_n$[d] | 17.1 | 33 |
| acetonitrile | – | 0.21 | 0.92 | 0.71 | 490 | 550 | 8.4 | 31 |
| methanol | 463 | 0.20 | 0.91 | 0.71 | 390 | 390 | 8.7 | this paper |
| | | | | | | 475 | 8.6 | |
| | | | | | | 630 | 8.5 | |

[a] $\lambda_{max}$ values correspond to the position of the maximum of the $S_0 \rightarrow S_2$ steady-state absorption spectrum in each solvent obtained from a Gaussian fit around the maximum. [b] The index of refraction $n$ and dielectric constant $\epsilon$ for the calculation of $\Delta f = R(\epsilon) - R(n)$ were taken from ref 38, with $R(\epsilon) = (\epsilon - 1)/(\epsilon + 2)$ and $R(n) = (n^2 - 1)/(n^2 + 2)$. [c] Only upper limits can be given for the time constant of the IC process $S_2 \rightarrow S_1$, where one typically finds $\tau_2(S_2 \rightarrow S_1) \leq 300$ fs. [d] "$S_1 \rightarrow S_n$" means that the probe wavelength was located on the $S_1 \rightarrow S_n$ band, but not explicitly reported.

Further insight into the steady-state spectroscopy of the three apocarotenals can be gained from their fluorescence spectra in solvents of different polarity, which also provide a comparison of the relative fluorescence amplitudes. The most striking feature of the spectra in *n*-hexane (Figure 3) is the change from $S_2 \rightarrow S_0$ fluorescence observed for 4′-apo-$\beta$-caroten-4′-al (conjugation length $N = 12$, see below) to predominantly $S_1 \rightarrow S_0$ emission for 12′-apo-$\beta$-caroten-12′-al ($N = 8$, see below). For the latter one, the $S_2 \rightarrow S_0$ fluorescence is still visible as a shoulder on the blue edge of the strong emission band, whereas the fluorescence spectrum of the former one almost resembles the mirror image of the $S_0 \rightarrow S_2$ absorption spectrum. Similar behavior has been observed for all-*trans*-apocarotenes,[37] apocarotenols,[41] unsubstituted polyenes,[42] spheroidenes,[43] and analogues of $\beta$-carotene,[44,45] where a relatively abrupt change in emission behavior occurred for carotenes with seven or eight conjugated bonds. This crossover from $S_2 \rightarrow S_0$ to $S_1 \rightarrow S_0$ fluorescence with decreasing conjugation length in nonpolar solvents can be explained by the increase of the time constant $\tau_1$ (i.e., decrease of the rate constant $k_1$) of $S_1 \rightarrow S_0$ internal conversion with increasing $S_1-S_0$ energy gap (see below), which results in a much higher quantum yield for $S_1 \rightarrow S_0$ fluorescence of 12′-apo-$\beta$-caroten-12′-al compared to 4′-apo-$\beta$-caroten-4′-al (provided that the radiative rate constants for the $S_1 \rightarrow S_0$ transition of the apocarotenals are comparable). The carotenoid 8′-apo-$\beta$-caroten-8′-al, shows a behavior more similar to 4′-apo-$\beta$-caroten-4′-al. For the 8′-species, the increasing importance of $S_1 \rightarrow S_0$ fluorescence is already signaled by the very weak fluorescence feature around 800 nm. Assuming that the radiative rate constant for $S_2 \rightarrow S_0$ fluorescence is comparable for the three apocarotenals, the similarity of the amplitudes of the $S_2 \rightarrow S_0$ fluorescence in all three spectra is consistent with experimental observations that the rate constant for the $S_2 \rightarrow S_1$ internal conversion step is always very small (on the order of 100 fs) and only weakly dependent on conjugation length.[2]

The fluorescence spectra in methanol (Figure 4) show a qualitatively similar behavior with respect to the change in conjugation length of the apocarotenal. This is a surprising observation. First of all, as will be discussed in detail below, for 12′-apo-$\beta$-caroten-12′-al in methanol, the IC process $S_1 \rightarrow S_0$ is accelerated by about a factor of 30 and is therefore close, e.g., to the IC rate constant of 4′-apo-$\beta$-caroten-4′-al in methanol. Assuming no change of the radiative rate constant, one would expect a massive drop of the $S_1 \rightarrow S_0$ fluorescence quantum yield so that the emission spectrum of 12′-apo-$\beta$-caroten-12′-al in methanol (Figure 4, bottom) should be more similar to that of 4′-apo-$\beta$-caroten-4′-al in the same solvent (Figure 4, top). However, a strong emission around 800 nm is observed for 12′-apo-$\beta$-caroten-12′-al in this highly polar solvent. This could be explained by the fact that the nature of the emissive state changes, such that its radiative rate constant becomes considerably larger. Indeed we have recently obtained an extensive set of transient pump−probe signals for 12′-apo-$\beta$-caroten-12′-al and 8′-apo-$\beta$-caroten-8′-al, where, after $S_2 \rightarrow S_1$ internal conversion, the formation of stimulated emission in the near IR region was detected, which was particularly strong in methanol. This is consistent with the formation of a state with substantial intramolecular charge-transfer character ("$S_1$/ICT"). We therefore believe that the fluorescence in the near IR region is due to such a state. Also, the maximum of the fluorescence is red-shifted with respect to that in *n*-hexane (Figure 3, bottom), which has been observed in other systems forming a charge transfer state from an initially locally excited state.[46,47] Several models have been suggested regarding the nature of such an "$S_1$/ICT" state in the case of peridinin. It was proposed that the $S_1$ state itself has ICT character.[15] Alternatively, polarity

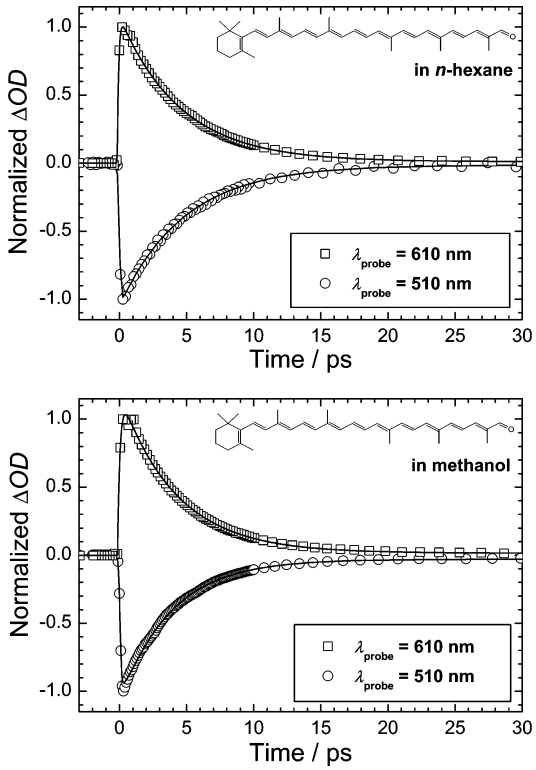


**Figure 5.** Normalized transient absorption signals of 4′-apo-β-caroten-4′-al after excitation to the $S_2$ state at 510 nm in *n*-hexane (top) and methanol (bottom). Open squares: $S_1$/ICT → $S_n$ absorption at 610 nm. Open circles: $S_0$ → $S_2$ absorption at 510 nm. Solid lines are fits using the model described in ref 32. Lifetimes see Table 1.

dependent mixing between the $S_1$ and ICT states could occur, resulting in a combined $S_1$/ICT state with varying degree of ICT character.[18] On the other hand, the presence of a distinct ICT state separated from the $S_1$ state has been also proposed.[16] Because this important question of the nature of the $S_1$ and ICT states is not yet completely understood, in the following we prefer to use the notation "$S_1$/ICT" to emphasize the likely involvement of an additional intramolecular charge transfer state in the intramolecular dynamics of the apocarotenals.

**Pump and Probe Wavelength Dependence of Transient Absorption Signals.** Representative experimental transient absorption signals for 4′-apo-β-caroten-4′-al in *n*-hexane and methanol are shown in Figure 5, where we plot the normalized ΔOD (eq 1) as a function of the temporal delay between the pump and probe pulses. The carotenoid was excited to the $S_2$ state at 510 nm which is close to the 0−0 transition of the $S_0$ → $S_2$ band, and the subsequent dynamics were probed at the wavelengths 510 nm (ground state recovery, GSR) and 610 nm (excited-state absorption, ESA). Additional time-resolved absorption traces have been obtained with the pump wavelength 480 nm at the absorption maximum (not shown here), and the time constants $\tau_1$ of the $S_1$/ICT → $S_0$ internal conversion process for all measurements in the solvents *n*-hexane, tetrahydrofuran and methanol are summarized in Table 1.

For 4′-apo-β-caroten-4′-al, the GSR signals at the probe wavelength 510 nm show an immediate drop at $t = 0$. Subsequently, the negative signal decays back to zero on a slower time scale. The fast initial drop is due to up-pumping of 4′-apo-β-caroten-4′-al to the $S_2$ state. After a very fast IC step $S_2$ → $S_1$/ICT, which typically occurs with a time constant $\tau_2 \leq$ 150 fs for most carotenoids,[2] the second IC step $S_1$/ICT → $S_0$ takes place resulting in a slower final recovery of the absorption signal. The signal can be analyzed in the framework of a simple kinetic model assuming two consecutive IC processes $S_2$ → $S_1$/ICT → $S_0$, with characteristic time constants $\tau_2$ ($=k_2^{-1}$) for the $S_2$ → $S_1$/ICT and $\tau_1$ ($=k_1^{-1}$) for the $S_1$/ICT → $S_0$ steps (where $k_2$ and $k_1$ are the corresponding rate constants). The full analytical solution for the set of kinetic equations, which also considers the finite time resolution of our setup, can be found in ref 32. Using this model, we determine $\tau_1$ to be 4.8 ps in *n*-hexane and 3.8 ps in methanol in the case of 4′-apo-β-caroten-4′-al. We estimate the uncertainties of the time constants $\tau_1$ to be smaller than ten percent. The probe wavelength 610 nm is located in the region where the ESA band $S_1$/ICT → $S_n$ of 4′-apo-β-caroten-4′-al is expected. Therefore the fast initial rise of the signal within our time resolution is due to formation of $S_1$/ICT state population by excitation of the molecules to the $S_2$ state and subsequent ultrafast IC. We can only give a rough estimate for this step of $\tau_2 \leq 300$ fs. The ESA profiles decay with the time constants $\tau_1(S_1/\text{ICT} \rightarrow S_0) = 4.6$ and 4.2 ps for *n*-hexane and methanol, respectively. These values are in excellent agreement with those extracted from the GSR profiles recorded at 510 nm. We find practically identical time constants for the pump wavelength 480 nm (see Table 1). Interestingly, all $\tau_1$ values for 4′-apo-β-caroten-4′-al are almost independent of solvent polarity. This is in contrast to our earlier measurements for the shorter 12′-apo-β-caroten-12′-al, which showed an almost 30-fold decrease of $\tau_1$ when going from *n*-hexane to methanol.[32]

We have also obtained transient absorption signals for 8′-apo-β-caroten-8′-al in *n*-hexane, tetrahydrofuran and methanol. In this case, the carotenoid was excited at 390 nm (blue edge of the $S_0$ → $S_2$ transition), and the subsequent dynamics were probed at the wavelengths 390, 475 (GSR), and 630 nm (ESA). Time constants $\tau_1$ for all measurements in the solvents *n*-hexane, tetrahydrofuran, and methanol are summarized in Table 1. Upon 390 nm excitation of 8′-apo-β-caroten-8′-al in *n*-hexane and tetrahydrofuran, a slight variation of the time constants with probe wavelength was observed in the range 21.0−25.4 ps. Two points can be made: first, $\tau_1$ values were generally larger in tetrahydrofuran and in *n*-hexane in all experimental data of probe wavelength dependence over the range 390−630 nm; second, upon excitation at 390 nm, $\tau_1$ was slightly larger at 475 nm.

The influence of the excitation wavelength on the $\tau_1$ values of 8′-apo-β-caroten-8′-al appears to be insignificant. Additional data sets for $\tau_1$ are also available from other groups,[29,31,33] where 8′-apo-β-caroten-8′-al was excited at 490 or 510 nm, which is close to the 0−0 transition of the $S_0$ → $S_2$ band: He et al.[31,33] obtained $\tau_1 = 26.4$ ps in 3-methylpentane after excitation at 490 nm (probed at 555 nm); similarly, Wasielewski et al. measured $\tau_1 = 25.1$ ps in toluene for excitation at 510 nm (probed at 480 nm).[29] There was no apparent influence of the excitation wavelength on the $\tau_1$ values. Within experimental error, these values are comparable to the 21−25 ps obtained by us in *n*-hexane.

In summary, it is rather difficult to draw clear conclusions for the excitation/probe wavelength dependence of the $\tau_1$ values of 8′-apo-β-caroten-8′-al, mainly because the change of $\tau_1$ is not as systematic as in the case of, e.g., the excitation wavelength dependence of peridinin lifetimes.[18] With respect to the slight variation of our $\tau_1$ values in *n*-hexane and tetrahydrofuran with probe wavelength, we can only speculate that the consecutive $S_2$ → $S_1$/ICT → $S_0$ IC scheme applied in the analysis has to be refined to account for all details of the dynamics, like, e.g., superimposed vibrational relaxation processes. Also, an ad-

ditional detailed spectral identification of transient species of 8′-apo-*β*-caroten-8′-al will be helpful.

**Solvent and Conjugation Length Dependence of the IC Time Constant $\tau_1$.** The GSR and ESA profiles of 8′-apo-*β*-caroten-8′-al are qualitatively similar to those obtained for 4′-apo-*β*-caroten-4′-al. The most striking difference however is the clear decrease of $\tau_1$ by a factor of 2.5 when going from *n*-hexane to methanol. Table 1 summarizes the polarity dependent IC time constants $\tau_1$ for 4′-apo-*β*-caroten-4′-al and 8′-apo-*β*-caroten-8′-al in *n*-hexane, tetrahydrofuran, and methanol. Corresponding values for 12′-apo-*β*-caroten-12′-al are available from our previous work.[32] The polarity is quantified in terms of the solvent polarity factor $\Delta f$ defined as

$$\Delta f = \frac{\epsilon - 1}{\epsilon + 2} - \frac{n^2 - 1}{n^2 + 2} \tag{3}$$

where values for the dielectric constant $\epsilon$ and index of refraction $n$ were taken from the literature.[38] Additional data of ultrafast transient absorption experiments for 8′-apo-*β*-caroten-8′-al are available from the earlier work of Kispert and Wasielewski.[29,31,33]

We observed a marked change of the solvent dependence when the conjugation length of the apocarotenal was shortened. The $\tau_1$ values for 4′-apo-*β*-caroten-4′-al were almost solvent independent, and the IC process was fast (4−5 ps). While in *n*-hexane and tetrahydrofuran the values were practically the same, a very mild reduction by about 0.5−1 ps (depending on probe wavelength) was observed in methanol. For 8′-apo-*β*-caroten-8′-al, the averaged values in *n*-hexane and tetrahydrofuran were very similar (22.7 and 24.4 ps) and dropped markedly only for the strongly polar methanol (8.6 ps) compared to 17.1 ps for the slightly less polar ethanol.[33] In contrast, 12′-apo-*β*-caroten-12′-al showed the largest variation of $\tau_1$ with solvent polarity: 220 ps (*n*-hexane), 91 ps (tetrahydrofuran), and 8 ps (methanol).[32] Apparently, there are characteristic differences regarding the onset and the strength of the solvent dependence of $\tau_1$ between the different apocarotenals. For instance, in the case of 12′-apo-*β*-caroten-12′-al, the data of the current work and pump−probe measurements in the near-infrared region in additional solvents suggest that in the lower polarity range ($\Delta f$ = 0−0.3) the $\tau_1$ values are not particularly sensitive to the solvent polarity. However, $\tau_1$ values are almost linearly correlated with $\Delta f$ over the range 0.3−0.7. While a qualitatively similar effect is also seen for 8′-apo-*β*-caroten-8′-al, the onset of solvent polarity dependence of $\tau_1$ appears at a higher $\Delta f$ value (ca. 0.6) compared to the 12′-species. Therefore, for 8′-apo-*β*-caroten-8′-al the values in *n*-hexane ($\Delta f = 0$) and tetrahydrofuran ($\Delta f = 0.44$) are very similar (e.g., 25.4 and 26.7 ps, respectively, at a probe wavelength of 475 nm), whereas for 12′-apo-*β*-caroten-12′-al a pronounced reduction is observed (averaged values of 220 vs 91 ps from ref 32). For 4′-apo-*β*-caroten-4′-al, $\tau_1$ is already very small in nonpolar solvents and in a range, where the values for the other two apocarotenals in methanol are located. The reason for the different behavior regarding the onset and the strength of polarity dependence for the three apocarotenals is not yet clear, but can be possibly rationalized in terms of varying $S_1-S_0$ and ICT$-S_0$ energy gaps (for details see below): For the longer conjugation lengths, the $S_1$ state might be already energetically so low that the stabilization of the ICT state has only a minor influence on the rate constant of internal conversion to $S_0$. In methanol, the similarity of the $\tau_1$ values for 12′-apo-*β*-caroten-12′-al and 8′-apo-*β*-caroten-8′-al might point toward similar ICT$-S_0$ energy gaps.

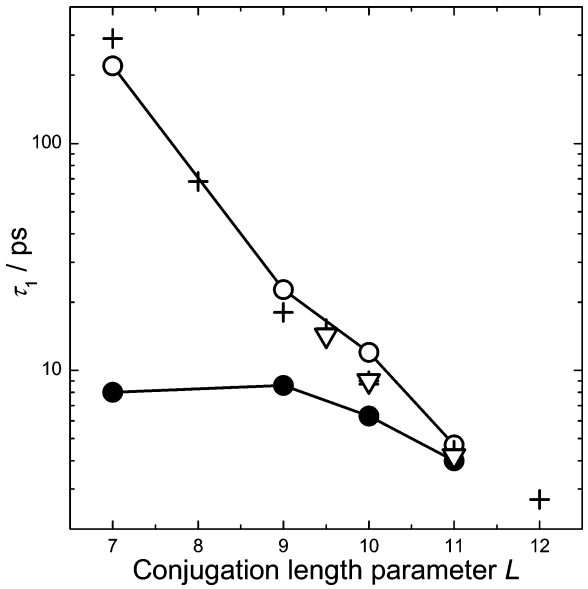


**Figure 6.** Internal conversion time constant $\tau_1$ as a function of the effective conjugation length for several carotenoids. Empirical conjugation length parameter $L = N_{chain} + 0.5 \cdot N_\beta + 0.5 \cdot N_{aldehyde}$ (see text). Open circles with lines, apocarotenals in *n*-hexane; filled circles with lines, apocarotenals in methanol. Crosses: carotenoids without C═O substitution in *n*-hexane (toluene in the case of lutein). Downward triangles: Carotenoids without C═O substitution in methanol. Lifetimes see Table 2. Lines connecting the apocarotenal data are only intended as a guide for the eye and have no further significance.

It is instructive to compare the $\tau_1$ results for the apocarotenals with data from earlier experiments for carotenoids without conjugated carbonyl groups as a function of conjugation length.[30−32,48−52] To do this, we introduced an empirical parameter $L$, which characterizes the effective conjugation length of the respective carotenoid:

$$L = N_{chain} + 0.5 \cdot N_\beta + 0.5 \cdot N_{aldehyde} \tag{4}$$

The empirical factor 0.5 was introduced in the second term to account for the experimental observation[2] that conjugated *β*-ionone C═C bonds are not fully conjugated with the rest of the system (resulting in a smaller effect on $\tau_1$ than a C═C double bond in a polyene chain would have). This is due to the fact, that the *β*-ionone ring is nonplanar, and therefore its C═C bond is not in plane with the rest of the polyene chain. Likewise the same factor 0.5 was introduced (empirically) in the third term, because it is known that replacing a C═C bond at the end of a polyene chain by a C═O group results in larger $\tau_1$ values in nonpolar solvents.[2] Using this definition, 12′-apo-*β*-caroten-12′-al had $L = 6 + 1 \cdot 0.5 + 1 \cdot 0.5 = 7$, whereas for *β*-carotene one obtained $L = 9 + 2 \cdot 0.5 + 0 = 10$.

The resulting correlation is presented in Figure 6, and corresponding $\tau_1$ values can be found in Table 2. Obviously, the $\tau_1$ results for the apocarotenals in nonpolar solvents (open circles with lines) fit very well into the correlation found for polyenes without aldehyde substituents (crosses). It should also be noted, that the $\tau_1$ values for unsubstituted carotenoids were independent of solvent polarity (crosses and triangles in Figure 6). This means that in nonpolar solvents apocarotenals showed the "expected" behavior when the conjugation length was changed. However the situation changed drastically when the apocarotenals were dissolved in a highly polar solvent like methanol (filled circles with lines in Figure 6). A pronounced reduction of $\tau_1$ in methanol relative to *n*-hexane (by a factor of 30) was observed for 12′-apo-*β*-caroten-12′-al. While the same

**TABLE 2: Comparison of the Lifetimes $\tau_1$ in Nonpolar and Highly Polar Solvents for 4′-apo-β-caroten-4′-al and 8′-apo-β-caroten-8′-al with Other Apocarotenals and Carotenoids**

| carotenoid | conjugation[a] | $L$[b] | $\tau_1$ (ps) (*n*-hexane) | $\tau_1$ (ps) (methanol) | ref |
|---|---|---|---|---|---|
| 4′-apo-β-caroten-4′-al | 10O1β1 | 11 | 4.7[c] | 4.0[c] | this paper |
| 6′-apo-β-caroten-6′-al | 9O1β1 | 10 | 12.0 | 6.3 | 31 |
| 8′-apo-β-caroten-8′-al | 8O1β1 | 9 | 22.7[c] | 8.6[c] | this paper |
| 12′-apo-β-caroten-12′-al | 6O1β1 | 7 | 220 | 8.0 | 32 |
| 7′,8′-didehydrospheroidene | 12 | 12 | 2.7 | − | 48 |
| rhodopin glucoside | 11 | 11 | − | 4.2 | 49 |
| lycopene | 11 | 11 | 4.7 | − | 50 |
| spheroidene | 10 | 10 | 8.7 | − | 48 |
| β-carotene | 9β2 | 10 | 9.0 | 9.0 | 30,51 |
| lutein | 9β1 | 9.5 | 15.3 (toluene) | 14.3 | 30 |
| nonaene | 9 | 9 | 18 | − | 52 |
| octaene | 8 | 8 | 68 | − | 52 |
| heptaene | 7 | 7 | 290 | − | 52 |
| peridinin | 7LOA | − | 161 | 12 | 7,9 |
| | | | 156 | 10.5 | 17 |

[a] Nomenclature see ref 2. [b] Empirical conjugation length parameter $L = N_{chain} + 0.5 \cdot N_{\beta} + 0.5 \cdot N_{aldehyde}$; see text. [c] Arithmetic averages of the respective values from Table 1.

qualitative trend was visible for 8′-apo-β-caroten-8′-al and 4′-apo-β-caroten-4′-al, the relative change became much smaller (factors of 2.6 and 1.2 for the 8′- and 4′-species, respectively). The large effect in 12′-apo-β-caroten-12′-al can be explained by the strong stabilization of the ICT state in highly polar solvents. The presence of such a state was also suggested by our very recent results from time-resolved pump−probe experiments in the near IR region, where after the first ultrafast $S_2 \rightarrow S_1$/ICT IC step a strong stimulated emission signal appeared for 12′-apo-β-caroten-12′-al in methanol, which decayed with practically the same time constant $\tau_1$ as reported earlier.[32] Interestingly, we also found stimulated emission in the near IR region for 8′-apo-β-caroten-8′-al in methanol. It was much weaker than for 12′-apo-β-caroten-12′-al and decayed with a time constant which was again very similar to the one already reported.[32] We also note that weak stimulated emission signals and therefore ICT-like behavior were even observed in nonpolar solvents for both 12′-apo-β-caroten-12′-al and 8′-apo-β-caroten-8′-al, which decayed with time constants very similar to those reported in the current study (ca. 220 and 21 ps, respectively). A tentative interpretation of this experimental evidence will be given below.

Finally, we note that the time constant $\tau_1$ of 8′-apo-β-caroten-8′-al in dichloromethane measured previously by He et al. is substantially lower than one would expect based on the polarity of this solvent alone ($\Delta f = 0.47$), which is similar to tetrahydrofuran ($\Delta f = 0.44$).[33] It is well-known that 8′-apo-β-caroten-8′-al can undergo electron transfer in chlorinated solvents and form radical cations, which absorb in the near IR region around 850 nm.[53] It is likely that such an additional intermolecular reactive channel is operative here, which leads to a reduction of $\tau_1$.

**Simplified Energy Gap Law Description of $S_1$/ICT IC Time Constants.** The apocarotenal series studied in this paper allows to gain additional insight into the influence of the polyene chain length on the intramolecular dynamics. Previously, this conjugation length dependence of the rate constant $k_1$ ($=\tau_1^{-1}$) of $S_1 \rightarrow S_0$ internal conversion has been successfully quantified using an energy gap law (EGL) approach[37,44,54−59]

$$k_1 = a \cdot \exp(-b \cdot \Delta E) \quad (5)$$

where in the simplest case $a$ and $b$ are constants, and $\Delta E$ is the $S_1-S_0$ energy gap. For shorter polyenes $\Delta E$ can be extrapolated from the (especially for substituted systems often not very well-resolved) fluorescence spectra of these weakly emitting species. The parameters $a$ and $b$ are also useful to estimate $S_1-S_0$ energy gaps for longer carotenoids (with more than nine conjugated double bonds), where fluorescence from the $S_1$ state is very weak (instead only $S_2 \rightarrow S_0$ fluorescence is mostly observed). Despite the apparent success of the EGL, caution should be exercised when applying it to a wide range of structurally different carotenoids, because its well-known that, in addition to the conjugation length, effects like the degree of methyl substitution or the number of β-ionone rings[37,41,60] result in slightly varying values for the parameters $a$ and $b$ in eq 5.[44,58,59] For the apocarotenals, we have to consider especially the influence of the carbonyl substituent, which results in the formation of considerable ICT contributions. Thus the observed fluorescence in the near IR region might be more generally denoted as an "$S_1$/ICT $\rightarrow S_0$" emission, particularly in polar solvents.

To compare our results with earlier EGL correlations, it is necessary to extract approximate energies for the 0−0 position of the $S_1 \rightarrow S_0$ electronic transition from our apocarotenal fluorescence spectra. In this respect, it is useful to draw a comparison with the results of Christensen et al., who carried out an extensive study of the emission spectra and $S_1-S_0$ energy gaps of the chemically related apocarotenes in EPA matrices at 77 K.[37] For instance, their results for 12′-apo-β-carotene (and also 10′-apo-β-carotene) suggest that the $S_1 \rightarrow S_0(0-0)$ transition of 12′-apo-β-caroten-12′-al can be identified with the shoulder of the fluorescence spectrum at 17750 $cm^{-1}$ (Figure 3, bottom). In the same way, considering the shape of their $S_1 \rightarrow S_0$ emission spectrum of 8′-apo-β-carotene it is reasonable to assume that the $S_0 \rightarrow S_1(0-0)$ transition of 8′-apo-β-caroten-8′-al should be located near the minimum of our fluorescence spectrum around 15200 $cm^{-1}$ (Figure 3, middle). For the longest of the apocarotenals, the 4′-species, such an extrapolation is no longer feasible, because of the very weak fluorescence in the range 700−800 nm.

An extensive set of available $S_1 \rightarrow S_0$ IC rate constants $k_1$ and energy gaps $\Delta E$ extracted from $S_1 \rightarrow S_0$ fluorescence spectra has been compiled by Frank et al. for 24 carotenoids.[56] In Figure 7 we compare their correlation (open circles) with our data for the apocarotenals in *n*-hexane (filled circles) in a semilogarithmic representation:

$$\ln(k_1/\mathrm{ps}^{-1}) = A - B \cdot \Delta E/\mathrm{cm}^{-1} \quad (6)$$

Applying a linear least-squares fit to the data of Franck's compilation (omitting their two points with the largest $\Delta E$)

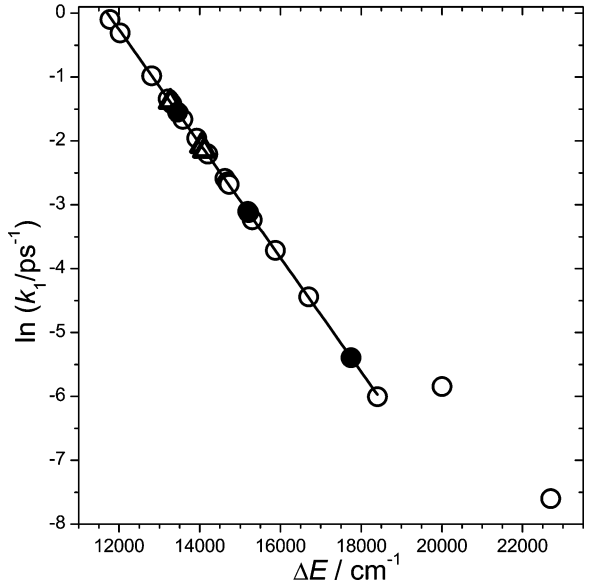


**Figure 7.** Semilogarithmic representation of the IC rate constant $k_1$ as a function of the $S_1$/ICT−$S_0$ energy gap $\Delta E$. Open circles, compilation from ref 56; solid line, linear fit to the data of ref 56 (eq 6) omitting the two points at largest $\Delta E$. Filled circles: apocarotenals in *n*-hexane (this work), where the energy gaps $\Delta E$ for 12′-apo-$\beta$-caroten-12′-al and 8′-apo-$\beta$-caroten-8′-al were determined from their fluorescence spectra, whereas for 4′-apo-$\beta$-caroten-4′-al a $\Delta E$ value of 13450 cm$^{-1}$ was extrapolated based on the linear fit and $k_1 = \tau_1^{-1}$ in Table 2. Open triangles: apocarotenals in methanol (this work), where all $\Delta E$ values were extrapolated using the linear fit and the time constants $\tau_1$ (see Table 2), yielding $\Delta E$ = 14040, 14120, and 13270 cm$^{-1}$, for the 12′-, 8′-, and 4′-species, respectively.

yields $A = \ln a = 10.45775$ and $B = 8.92873 \cdot 10^{-4}$ (solid line in Figure 7). Our data for 12′-apo-$\beta$-caroten-12′-al and 8′-apo-$\beta$-caroten-8′-al are in very good agreement with this correlation. Similar to the conclusions drawn from Figure 6, this supports the interpretation that apocarotenals in nonpolar solvents show the expected conjugation length dependence of their $S_1$ lifetimes. Using the above correlation we can also predict the $S_1-S_0$ energy gap for 4′-apo-$\beta$-caroten-4′-al in *n*-hexane to be $\Delta E$ = 13450 cm$^{-1}$.

In the case of methanol an analogous correlation of the $S_1-S_0$ energy gap with the shape of the fluorescence spectra is no longer successful. As an example, applying a similar procedure as outlined above to the 12′-apo-$\beta$-caroten-12′-al fluorescence spectrum (Figure 4, bottom) would yield $\Delta E$ = 16200 cm$^{-1}$, which is far off from the correlation in Figure 7. If the EGL correlation would be valid, one would instead expect $\Delta E$ values of 14040, 14120, and 13270 cm$^{-1}$ for the 12′-, 8′-, and 4′-species, respectively (open triangles in Figure 7). This could be simply due to a failure of the EGL approach for carotenoid systems having ICT contributions. However, it could also mean that ICT contributions to the $S_1$/ICT fluorescence spectrum, especially for 12′-apo-$\beta$-caroten-12′-al in methanol (Figure 4, bottom), mainly arise from energies around the maximum of the fluorescence emission. The latter interpretation would be also consistent with a preliminary analysis of time-resolved ICT stimulated emission data recorded by us very recently, which show that stimulated emission yields are highest above 800 nm and tail off toward 740 nm.

## 4. Conclusions

We have presented femtosecond pump−probe transient absorption measurements of the ultrafast internal conversion processes of a series of apocarotenals with varying conjugation length in different solvents. 4′-apo-$\beta$-caroten-4′-al having the largest number of conjugated double bonds shows the smallest time constant (largest IC rate constant) for the $S_1$/ICT → $S_0$ transition, and in this case $\tau_1$ is almost independent of solvent polarity (ca. 5 ps in *n*-hexane and 4 ps in methanol). For the shorter 8′-apo-$\beta$-caroten-8′-al, a pronounced reduction of $\tau_1$ from 22.7 to 8.6 ps was observed when changing from *n*-hexane to methanol, which is however still much weaker than previously reported for the even shorter 12′-apo-$\beta$-caroten-12′-al (220 and 8.0 ps, respectively).[32] The conjugation length dependence of $\tau_1$ in the nonpolar solvent *n*-hexane can be described by an energy gap law approach based on $S_1-S_0$ energy differences obtained from the evaluation of the static fluorescence spectra of the apocarotenals. In highly polar solvents like methanol the IC process is very fast, and only weakly dependent on the conjugation length. Based on our experimental findings the following (tentative) picture of the excited-state dynamics of apocarotenals appears to be reasonable: For apocarotenals with short conjugation length (and thus a long $S_1$ lifetime in nonpolar solvents) an ICT state is strongly stabilized in highly polar solvents resulting in a large reduction of the lifetime. For apocarotenals with long conjugation length, the lifetime of the $S_1$ state is already very short in nonpolar solvents, so the influence of ICT character on the lifetime appears to become less and less important with increasing conjugation length.

**Acknowledgment.** Financial support by the Alexander von Humboldt foundation within the "Sofja Kovalevskaja Program" and by the German Science Foundation is gratefully acknowledged. We would like to thank T. Polívka, J. Troe, K. Luther, D. Schwarzer, J. Schroeder, M. Kopczynski, S. Kühn and C. Reichardt for stimulating discussions. Some of the fluorescence data were provided by J. Seehusen. Special thanks go to the BASF AG, and here especially H. Ernst, for generously providing the all-*trans*-apo-$\beta$-carotenal samples and extensive advice. We also thank J. Schimpfhauser and J. Bienert for the purification of the all-*trans*-4′-apo-$\beta$-caroten-4′-al sample.

## References and Notes

(1) In *The Photochemistry of Carotenoids*; Frank, H. A., Young, A. J., Britton, G., Cogdell, R. J., Eds.; Kluwer: Dordrecht, The Netherlands, 1999.

(2) Polívka, T.; Sundström, V. *Chem. Rev.* **2004**, *104*, 2021.

(3) Holt, N. E.; Zigmantas, D.; Valkunas, L.; Li, X.-P.; Niyogi, K. K.; Fleming, G. R. *Science* **2005**, *307*, 433.

(4) Goodwin, T. W. *The Biochemistry of Carotenoids*, 2 ed.; Chapman & Hall: London, 1980; Vol. 1.

(5) Liaaen-Jensen, S. In *Carotenoids*; Britton, G., Liaaen-Jensen, S., Pfander, H., Eds.; Birkhäuser Verlag: Berlin, 1998; Vol. 3, p 217.

(6) Johansen, J. E.; Svec, W. A.; Liaaen-Jensen, S.; Haxo, F. T. *Phytochemistry* **1974**, *13*, 2261.

(7) Frank, H. A.; Bautista, J. A.; Josue, J.; Pendon, Z.; Hiller, R. G.; Sharples, F. P.; Gosztola, D.; Wasielewski, M. R. *J. Phys. Chem. B* **2000**, *104*, 4569.

(8) Hiller, R. G. Carotenoids as Components of the Light-harvesting Proteins of Eukaryotic Algae. In *The Photochemistry of Carotenoids*; Frank, H. A., Young, A. J., Britton, G., Cogdell, R. J., Eds.; Kluwer: Dordrecht, The Netherlands, 1999; p 81.

(9) Bautista, J. A.; Connors, R. E.; Raju, B. B.; Hiller, R. G.; Sharples, F. P.; Gosztola, D.; Wasielewski, M. R.; Frank, H. A. *J. Phys. Chem. A* **1999**, *103*, 8751.

(10) Bautista, J. A.; Hiller, R. G.; Sharples, F. P.; Gosztola, D.; Wasielewski, M. R.; Frank, H. A. *J. Phys. Chem. A* **1999**, *103*, 2267.

(11) Papagiannakis, E.; Larsen, D. S.; van Stokkum, I. H. M.; Vengris, M.; Hiller, R. G.; van Grondelle, R. *Biochemistry* **2004**, *43*, 15303.

(12) Papagiannakis, E.; Vengris, M.; Larsen, D. S.; van Stokkum, I. H. M.; Hiller, R. G.; van Grondelle, R. *J. Phys. Chem. B* **2006**, *110*, 512.

(13) Polívka, T.; Pascher, T.; Sundström, V.; Hiller, R. G. *Photosynth. Res.* **2005**, *86*, 217.

(14) Premvardhan, L.; Papagiannakis, E.; Hiller, R. G.; van Grondelle, R. *J. Phys. Chem. B* **2005**, *109*, 15589.

(15) Shima, S.; Ilagan, R. P.; Gillespie, N.; Sommer, B. J.; Hiller, R. G.; Sharples, F. P.; Frank, H. A.; Birge, R. R. *J. Phys. Chem. A* **2003**, *107*, 8052.
(16) Vaswani, H. M.; Hsu, C.-P.; Head-Gordon, M.; Fleming, G. R. *J. Phys. Chem. B* **2003**, *107*, 7940.
(17) Zigmantas, D.; Polívka, T.; Hiller, R. G.; Yartsev, A.; Sundström, V. *J. Phys. Chem. A* **2001**, *105*, 10296.
(18) Zigmantas, D.; Hiller, R. G.; Yartsev, A.; Sundström, V.; Polívka, T. *J. Phys. Chem. B* **2003**, *107*, 5339.
(19) Sashima, T.; Koyama, Y.; Yamada, T.; Hashimoto, H. *J. Phys. Chem. B* **2000**, *104*, 5011.
(20) Koyama, Y.; Rondonuwu, F. S.; Fujii, R.; Watanabe, Y. *Biopolymers* **2004**, *74*, 2.
(21) Cerullo, G.; Polli, D.; Lanzani, G.; De Silvestri, S.; Hashimoto, H.; Cogdell, R. J. *Science* **2002**, *298*, 2395.
(22) Larsen, D. S.; Papagiannakis, E.; van Stokkum, I. H. M.; Vengris, M.; Kennis, J. T. M.; van Grondelle, R. *Chem. Phys. Lett.* **2003**, *381*, 733.
(23) Gradinaru, C. C.; Kennis, J. T. M.; Papagiannakis, E.; van Stokkum, I. H. M.; Cogdell, R. J.; Fleming, G. R.; Niederman, R. A.; van Grondelle, R. *Proc. Natl. Acad. Sci. U.S.A.* **2001**, *98*, 2364.
(24) Wohlleben, W.; Buckup, T.; Herek, J. L.; Cogdell, R. J.; Motzkus, M. *Biophys. J.* **2003**, *85*, 442.
(25) Wohlleben, W.; Buckup, T.; Hashimoto, H.; Cogdell, R. J.; Herek, J. L.; Motzkus, M. *J. Phys. Chem. B* **2004**, *108*, 3320.
(26) Billsten, H. H.; Pan, J.; Sinha, S.; Pascher, T.; Sundström, V.; Polívka, T. *J. Phys. Chem. A* **2005**, *109*, 6852.
(27) Papagiannakis, E.; van Stokkum, I. H. M.; Vengris, M.; Cogdell, R. J.; van Grondelle, R.; Larsen, D. S. *J. Phys. Chem. B* **2006**, *110*, 5727.
(28) Christensen, R. L.; Barney, E. A.; Broene, R. D.; Galinato, M. G. I.; Frank, H. A. *Arch. Biochem. Biophys.* **2004**, *430*, 30.
(29) Wasielewski, M. R.; Kispert, L. D. *Chem. Phys. Lett.* **1986**, *128*, 238.
(30) Kopczynski, M.; Lenzer, T.; Oum, K.; Seehusen, J.; Seidel, M. T.; Ushakov, V. G. *Phys. Chem. Chem. Phys.* **2005**, *7*, 2793.
(31) He, Z.; Gosztola, D.; Deng, Y.; Gao, G.; Wasielewski, M. R.; Kispert, L. D. *J. Phys. Chem. B* **2000**, *104*, 6668.
(32) Wild, D. A.; Winkler, K.; Stalke, S.; Oum, K.; Lenzer, T. *Phys. Chem. Chem. Phys.* **2006**, *8*, 2499.
(33) He, Z.; Kispert, L. D.; Metzger, R. M.; Gosztola, D.; Wasielewski, M. R. *J. Phys. Chem. B* **2000**, *104*, 6302.
(34) Piel, J.; Beutter, M.; Riedle, E. *Opt. Lett.* **2000**, *25*, 180.
(35) Riedle, E.; Beutter, M.; Lochbrunner, S.; Piel, J.; Schenkl, S.; Spörlein, S.; Zinth, W. *Appl. Phys. B* **2000**, *71*, 457.
(36) Wilhelm, T.; Piel, J.; Riedle, E. *Opt. Lett.* **1997**, *22*, 1494.
(37) Christensen, R. L.; Goyette, M.; Gallagher, L.; Duncan, J.; DeCoster, B.; Lugtenburg, J.; Jansen, F. J.; van der Hoef, I. *J. Phys. Chem. A* **1999**, *103*, 2399.
(38) *Handbook of Chemistry and Physics*, 85 ed.; CRC Press: Boca Raton, FL, 2004.
(39) Chen, Z.; Lee, C.; Lenzer, T.; Oum, K. *J. Phys. Chem. A* **2006**, *110*, 11291.
(40) O'Neil, M. P.; Wasielewski, M. R.; Khaled, M. M.; Kispert, L. D. *J. Chem. Phys.* **1991**, *95*, 7212.
(41) Cosgrove, S. A.; Guite, M. A.; Burnell, T. B.; Christensen, R. L. *J. Phys. Chem.* **1990**, *94*, 8118.
(42) Snyder, R.; Arvidson, E.; Foote, C.; Harrigan, L.; Christensen, R. L. *J. Am. Chem. Soc.* **1985**, *107*, 4117.
(43) DeCoster, B.; Christensen, R. L.; Gebhard, R.; Lugtenburg, J.; Farhoosh, R.; Frank, H. A. *Biochem. Biophys. Acta* **1992**, *1102*, 107.
(44) Andersson, P. O.; Bachilo, S. M.; Chen, R.-L.; Gillbro, T. *J. Phys. Chem.* **1995**, *99*, 16199.
(45) Andersson, P. O.; Gillbro, T.; Asato, A. E.; Liu, R. S. H. *J. Luminescence* **1992**, *51*, 11.
(46) Demeter, A.; Bérces, T.; Zachariasse, K. A. *J. Phys. Chem. A* **2001**, *105*, 4611.
(47) Grabowski, Z. R.; Rotkiewicz, K.; Rettig, W. *Chem. Rev.* **2003**, *103*, 3899.
(48) Frank, H. A.; Desamero, R. Z. B.; Chynwat, V.; Gebhard, R.; van der Hoef, I.; Jansen, F. J.; Lugtenburg, J.; Gosztola, D.; Wasielewski, M. R. *J. Phys. Chem. A* **1997**, *101*, 149.
(49) Polívka, T.; Zigmantas, D.; Herek, J. L.; He, Z.; Pascher, T.; Pullerits, T.; Cogdell, R. J.; Frank, H. A.; Sundström, V. *J. Phys. Chem. B* **2002**, *106*, 11016.
(50) Fujii, R.; Onaka, K.; Nagae, H.; Koyama, Y.; Watanabe, Y. *J. Luminescence* **2001**, *92*, 213.
(51) Billsten, H. H.; Zigmantas, D.; Sundström, V.; Polívka, T. *Chem. Phys. Lett.* **2002**, *355*, 465.
(52) Frank, H. A.; Josue, J. S.; Bautista, J. A.; van der Hoef, I.; Jansen, F. J.; Lugtenburg, J.; Wiederrecht, G.; Christensen, R. L. *J. Phys. Chem. B* **2002**, *106*, 2083.
(53) Ding, R.; Grant, J. L.; Metzger, R. M.; Kispert, L. D. *J. Phys. Chem.* **1988**, *92*, 4600.
(54) Englman, R.; Jortner, J. *Mol. Phys.* **1970**, *18*, 145.
(55) Freed, K. F. *Acc. Chem. Res.* **1978**, *11*, 74.
(56) Frank, H. A.; Chynwat, V.; Desamero, R. Z. B.; Farhoosh, R.; Erickson, J.; Bautista, J. *Pure Appl. Chem.* **1997**, *69*, 2117.
(57) Frank, H. A.; Farhoosh, R.; Gebhard, R.; Lugtenburg, J. *Chem. Phys. Lett.* **1993**, *207*, 88.
(58) Chynwat, V.; Frank, H. A. *Chem. Phys.* **1995**, *194*, 237.
(59) Bachilo, S. M.; Spangler, C. W.; Gillbro, T. *Chem. Phys. Lett.* **1998**, *283*, 235.
(60) Bouwman, W. G.; Jones, A. C.; Phillips, D.; Thibodeau, P.; Friel, C.; Christensen, R. L. *J. Phys. Chem.* **1990**, *94*, 7429.